LBL-12814

CONF-810376--3

Lawrence Berkeley Laboratory

UNIVERSITY OF CALIFORNIA

Physics, Computer Science & Mathematics Division

Presented at the XVIth Rencontre de Moriond, Elementary Particle Physics Meetings, Les Arcs, Savo , France, March 15-27, 1981

ELASTIC AND INELASTIC ψ PRODUCTION BY MUONS

Stewart C. Loken

June 1981

Prepared for the U.S. Department of Energy under Contract W-7405-ENG-48

ELASTIC AND INELASTIC ψ PRODUCTION BY MUONS

Stewart C. Loken
Lawrence Berkeley Laboratory
University of California
Berke'ey, CA 94720

Presented at the XVIth Rencontre de Moriond,
Elementary Particle Physics Meetings, Les Arcs, Savoie, France,
March 15-27, 1981.

June 1981

This work was supported by the High Energy Physics Division of the U.S. Department of Energy under Contract No. W-7405-ENG-48.

ELASTIC AND INELASTIC ψ PRODUCTION BY MUONS

Stewart C. Loken
Lawrence Berkeley Laboratory
University of California
Berkeley, CA 94720

ABSTRACT

We present results on the elastic and inelastic production of ψ (3.1). The elastic data are qualitative agreement with the predictions of photon-gluon fusion but have a steeper dependence on Q^2 than the model predicts. A QCD calculation accounts well for the shape of the inelastic data in inelasticity, Q^2 and E_γ, but fails to account for the absolute cross section. At 209 GeV, the cross-section for elastic ψ production is 0.36±0.07nb; for inelastic, 0.28±0.06nb.

RESUME

Nous présentont de nouvelles données sur la production élastique at inélastique de ψ(3.1). La distribution des ψ élastique confirme en général les predictions du modele de fusion photon-gluon mais apparait plus pentue en Q^2 que l'on attend de la modèle. Une calculation de QCD rend compte des distributions de ψ inélastique mais pas la section efficace. A 209 GeV, les sections efficaces de production élastique at inélastique sont respectivement 0.36±0.07nb et 0.28±0.06nb.

A. Introduction

The Berkeley-Fermilab-Princeton Collaboration[1] has used the Multimuon spectrometer at Fermilab to study single and multimuon final states in high energy muon scattering. Data taken in early 1978 provided the first measurement of the cross section for charm muoproduction and its role in scale noninvariance of the nucleon structure function.[2] The experiment also provided limits on the mass of heavy neutral and doubly charged muons.[3] The study of high mass dimuon pairs has set a limit on the muoproduction of T.[4]

The apparatus and analysis method have been described elsewhere.[5] In this paper we discuss the production of the $\psi(3.1)$ by muons. We describe recent results on elastic ψ production in Section B. In Section C, we present new results on the inelastic production of ψ (3.1). Section D summarizes the cross sections for ψ production by muons.

B. Elastic ψ Production

We present fits of our data to the predictions of the photon-gluon fusion model.[6] In general, $R=\sigma_L/\sigma_T$ can depend on Q^2. Any Q^2 dependence in the angular distribution, together with non-uniform angular acceptance of the spectrometer can bias the interpretation of the overall Q^2 distribution.

To study these effects we have made simultaneous fits to an angular function and a Q^2 dependence of the form $(1+Q^2/\Lambda^2)^{-2}$. To allow for the possibility of Q^2 dependence of nuclear screening the fits were made with a screening factor included or ignored.[7] The details of this analysis have been published for elsewhere.[8]

The Q^2 dependence of σ_{eff} $(\mu Fe \rightarrow \psi X)$ is presented in Figure 1. Our insensitivity to the exact form of R and to the possible nuclear shadowing results in a propagator mass Λ between 1.9 and 2.6 GeV/c . A mass $\Lambda=m\psi$ is ruled out. A fit to the Q^2 projection indicates that the data fall faster than predicted by the photon-gluon-fusion model (γGF).

To study in more detail the validity of the photon-gluon-fusion model, we have performed simultaneous fits to the Q^2 and E_γ dependence of the data. In these fits we vary the effective charm quark mass m_c defined by the propagator

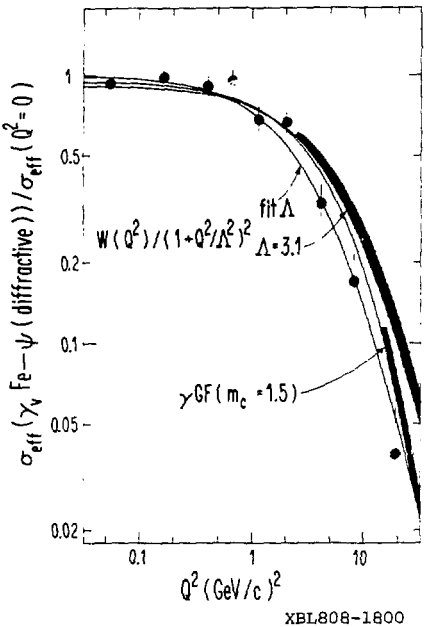

Figure 1. Q^2 dependence of the effective cross section for the reaction $\mu Fe \to \psi X$ (energy of X ~4.5 GeV). Statistical errors are shown. Typical Q^2 resolution is 3.1 (0.6) $(GeV/c)^2$ at Q^2=1.7 (1.2) $(GeV/c)^2$. The data are filled to $(1+Q^2/\Lambda^2)^{-2}$ multiplied by an angular function W. The best fits with free Λ and fixed Λ=3.1 are shown. Also exhibited is the prediction of γGF. At high Q^2, the γGF prediction and fixed fit are displayed as a solid band with the upper (lower) edge including (omitting) the nuclear screening factor.

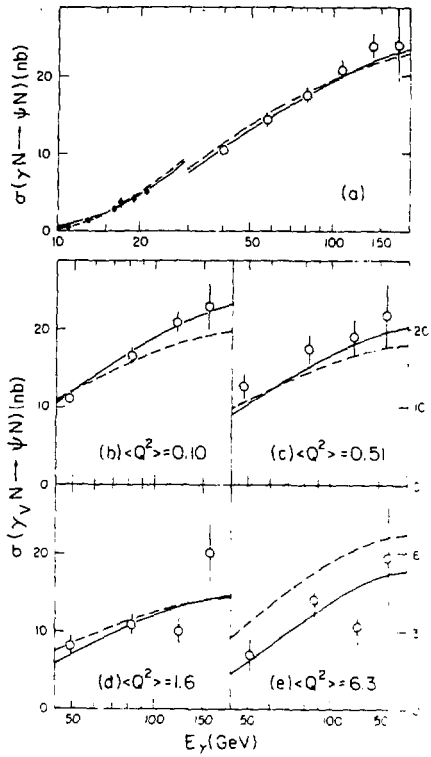

Figure 2. Energy dependence of the cross section for diffractive ψ production. 2a displays the data from this experiment (open circles) corrected to Q^2=0. The solid circles are data from a SLAC ψ photoproduction experiment. The dashed and solid curves respectively indicate γGF fits with the value n of the exponent in xG(x) fixed (n=5) and determined by the data (n=5.3±0.4). The relative normalization of the two experiments is allowed to vary within the quoted systematic errors. 2b, c, d, and e are the data from this experiment bined in Q^2 as indicated. The dashed curve is the prediction of standard γGF. The solid line is the best fit to the data giving m_c=1.08±.07 and n=8.6±1.1.

mass ($\Lambda=2m_c$), and the exponent n in the gluon distribution $xG(x)=(1-x)^n$. These fits are compared with predictions of the standard γGF $m_c=1.5 GeV/c^2$ and n=5.

Figure 2 b-e presents the results of these fits. Standard γGF is a good fit to the data at low Q^2 but fails to predict the cross section at high Q^2. The best fit to all data gives an effective mass $m_c=1.08\pm.07$ with the exponent of the gluon distribution $n=8.6\pm1.1$. Figure 2a we display the data extrapolated to $Q^2=0$. Also shown are data from a low energy photoproduction experiment.[9] The standard γGF agrees well with the data from both experiments. Allowing n to vary, the fit value is 5.3 ± 0.4.

C. Inelastic ψ Production

We define inelastic events by the energy measured in the hadron calorimeter ($E(X)>4.5$ GeV). For the purposes of this analysis we consider three regions of inelasticity $Z=E\psi/E\gamma$. (Figure 3).

The region $0.9<Z<1.0$ corresponds to small values of calorimeter energy. Because of radiative corrections, energy loss fluctuations, and calorimeter resolution, there is a large contribution from elastic events. In addition, the modeling of acceptance and analysis efficiency in this region is subject to significant systematic uncertainties. We exclude this region from the analysis.

In addition to inelastic ψ production, we expect to see contributions from elastic production of ψ' and χ states through their decays to ψ. Because of the small mass separations, these states will populate the region $0.7<Z<0.9$. The expected ψ' contribution is shown in Figure 3; states with smaller mass splitting from the ψ would be shifted to higher values of Z.

The region $Z<0.7$ contains only inelastic events. The inelastic process has been studied by Berger and Jones[10] using a two gluon model. The results of their calculation are compared with our data in Figure 3. It should be noted that the model does not include the ψ' cascades.

The Q^2-dependence of $\sigma_{eff}(\mu Fe\rightarrow\psi X)$ is shown in Figure 4. The data from the two regions of Z are consistent. The propagator masses of 2.6 ± 0.2, and 3.1 ± 0.4 are larger than that observed for elastic ψ production. This result contradicts that of the European Muon Collaboration (EMC).

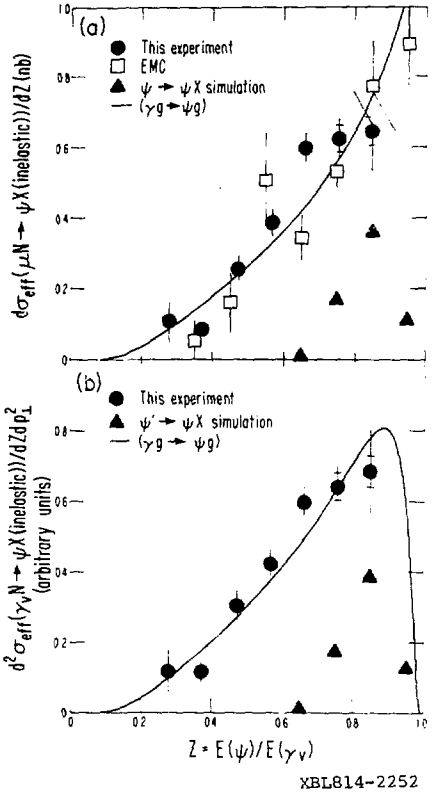

Figure 3. Dependence of the effective cross section for ψ production on inelasticity Z. 3a compares the data from this experiment with those of the European Muon Collaboration (EMC) and with the prediction of the two gluon model. The triangles indicate the expected event population from elastic events in which the ψ' decays to the ψ. 3b compares the differential cross section ($d\sigma/dzdp^2$) with the prediction of the two gluon model. For $Z<0.7$ statistical errors are shown. For $0.7<Z<0.9$, estimated systematic errors have been added in quadrature with the statistical errors whose magnitude is indicated by the cross-hatches.

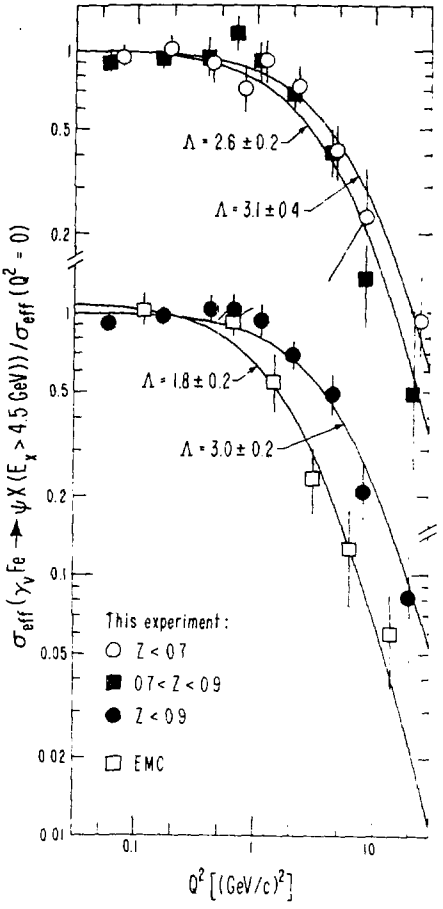

Figure 4. Q^2 dependence of the effective cross section for the reaction $\mu Fe \rightarrow \psi X$ (Energy of $X>4.5$ GeV). Statistical errors are shown. The upper portion compares data from this experiment in the two regions of inelasticity. The data are fitted to $(1+Q^2/\Lambda^2)^{-2}$. In the lower portion, data with $Z<0.9$ are fit to the same form with $\Lambda=3.0\pm0.2$. The open squares are the results of the EMC for all $Z<1.0$.

Figure 5 displays the cross section as a function of photon energy. The data are in good agreement with the shape predicted by Berger and Jones although their model fails to predict the magnitude of the cross section The data are also consistent with the shape of the elastic data. The preliminary EMC data showed a very steep energy dependence which is inconsistent with the present result.

D. Muon Cross-sections

From the data described above, we have determined the cross section for production by 215 GeV muons.

$$\sigma_{\text{elastic}} \quad (\mu N \rightarrow \psi X) = 0.36 \text{ nb} \pm 0.07$$

$$\sigma_{\text{inelastic}} \quad (\mu N \rightarrow \psi X) = 0.28 \text{ nb} \pm 0.05$$

$$\sigma_{\text{total}} \quad (\mu N \rightarrow \psi X) = 0.64 \text{ nb} \pm 0.13$$

The errors are dominated by systematic uncertainties at the 20% level. In the final error analysis, we expect the error on the total cross section to be significantly smaller.

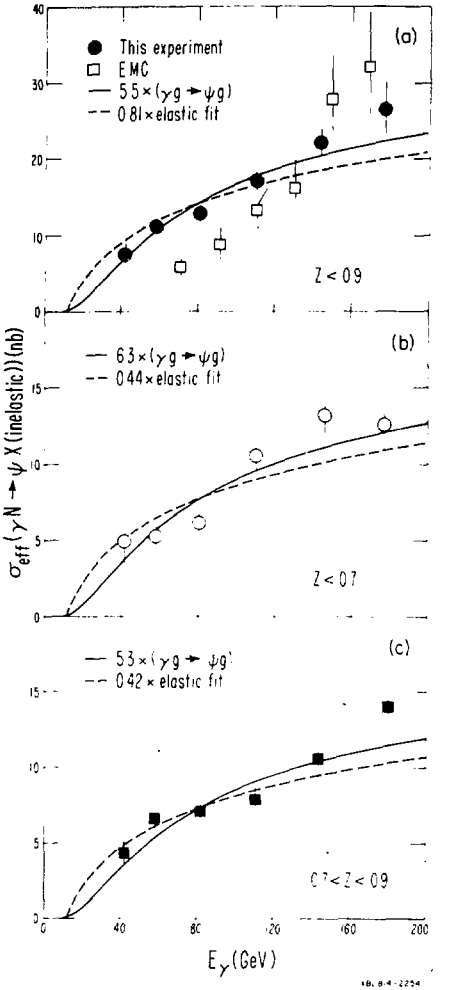

Figure 5. Energy dependence of the effective cross section for inelastic ψ production. 5b and c present data with statistical errors for $Z<0.7$ and $0.7<Z<0.9$ respectively. 5a presents the combined data $Z<0.9$. The dashed curve is a fit to the elastic data, normalized independently for each region of inelasticity. The solid curve is the prediction of Berger and Jones, normalized for each region. The EMC results (open squares) have been multiplied by a factor 0.73 to account for the fact that the EMC includes all Z whereas this experiment has restricted the data to $Z<0.9$. The factor 0.73 is the fraction of the EMC data with $Z<0.9$.

References:

1. A.R. Clark, K.J. Johnson, L.T. Kerth, S.C. Loken, T.W. Markiewicz, P.D. Meyers, W.H. Smith, M. Strovink, and W.A. Wenzel, Physics Department and Lawrence Berkeley Laboratory, University of California, Berkeley, CA. R.P. Johnson, C. Moore, M. Mugge, and R.E. Shafer, Fermi National Accelerator Laboratory, Batavia, IL. G.D. Gollin, F.C. Shoemaker, and P. Surko, Joseph Henry Laboratories. Princeton University, Princeton, NJ.

2. A.R. Clark et al. Phys. Rev. Lett 45, 682 (1980); A.R. Clark et al. Phys. Rev. Lett. 45, 1465 (1980); G.D. Gollin et al. LBL-12086, to be published in Phys. Rev. D.

3. A.R. Clark et al. Phys. Rev. Lett. 46, 299 (1981).

4. A.R. Clark et al. Phys. Rev. Lett. 45, 686 (1980).

5. A.R. Clark et al. Phys. Rev. Lett. 43, 187 (1979).

6. J.P. Leveille and T. Weiler, Nucl. Phys. B147, 147 (1979) and references cited therein.

7. H. Miettinen, presented at the XX International Conference on High Energy Physics, Madison, Wisconsin, July 17-23, 1980.

8. A.R. Clark et al. Phys. Rev. Lett. 45, 2092 (1980).

9. U. Camerini et al. Phys. Rev. Lett. 35, 483 (1975).

10. Edmond L. Berger and D. Jones, ANL-HEP-PR-80-72. To be published (1980).

11. R.P. Mount. Proceedings of the XX International Conference on High Physics, Loyal Durand and Lee G. Pondrom ed., 205 (1981).

Supported by the High Energy Physics Division of the U.S. Department of Energy under Contract No. W-7405-ENG-48.